

# An Improved Tail Current Source for Low Voltage Applications

Fan You, Sherif H. K. Embabi, *Member, IEEE*, J. Francisco Duque-Carrillo, *Member, IEEE*, and Edgar Sánchez-Sinencio, *Fellow, IEEE*

**Abstract**—A new current source for low-voltage applications is proposed. This current source is well suited for biasing differential pairs and source followers. Measured compliance voltage is slightly smaller than that of a single transistor. Its output resistance is a factor of 25 larger than that of a single transistor current source and was measured to be 8 M $\Omega$ . The use of the new current source improves the common-mode input range and the common-mode rejection ratio of fully balanced and single-ended differential amplifiers.

**Index Terms**—Analog circuits, current source, low voltage.

## I. INTRODUCTION

THE demand for analog circuits which can operate at low voltage is an established fact and does not need any further justification. An ideal current source is a two-terminal element with a parallel resistance  $R_{out}$  which is ideally infinite. Traditional current sources, such as simple, cascode, and regulated cascode [1] current sources (see Table I), suffer from a tradeoff between the output resistance and the compliance voltage (the minimum voltage required for the current source to operate). Other topologies such as the generalized cascode [2] and the active regulated cascode [3] have improved  $R_{out}$  with a relatively low compliance voltage of  $2V_{DSsat}$ . This, however, may still be too large to be tolerated in low voltage circuits. For example, in differential amplifiers, the compliance voltage of the tail current source must be minimal to maximize the input common-mode range (CMR). Krenik *et al.* [4] proposed a current source which has a high output resistance and its compliance voltage is one  $V_{DSsat}$ . This circuit is also suitable for biasing low-voltage differential pairs. It requires an added replica differential pair which is used to sense the current in the original input differential pair. This, however, increases the noise level.

In this paper, we are proposing a low-voltage (LV) current source structure which offers both the low compliance voltage and the high output resistance [5]. The proposed approach is

Manuscript received June 22, 1996; revised March 7, 1997. This work was supported in part by a grant from the Mixed Signal Products Group at Texas Instruments, Inc. The work of J. F. Duque-Carrillo was supported by R&D Spanish Plan (Grant TIC-94-0616).

F. You was with the Department of Electrical Engineering, Texas A&M University, College Station, TX 77843-3128 USA. He is now with Bell Labs, Lucent Technologies, Allentown, PA 18103 USA.

S. H. K. Embabi and E. Sánchez-Sinencio are with the Department of Electrical Engineering, Texas A&M University, College Station, TX 77843-3128 USA.

J. F. Duque-Carrillo is with the Department of Electronics, University of Extremadura, Badajoz, Spain.

Publisher Item Identifier S 0018-9200(97)05305-5.

TABLE I  
COMPARISON BETWEEN CURRENT SOURCE TOPOLOGIES

Current Source Type	$R_{out}$	$V_{compliance}$
Simple	$r_o$	$V_{DSsat}$
Cascode	$r_o^2 g_m$	$2V_{DSsat} + V_T$
Regulated Cascode [1]	$r_o^3 g_m^2$	$2V_{DSsat} + V_T$
Generalized Cascode [2]	$r_o^2 g_m$	$2V_{DSsat}$
Active Regulated Cascode [3]	$A r_o^2 g_m$	$2V_{DSsat}$
This Work	$r_o^2 g_m$	$V_{DSsat}$

$r_o$  is the output resistance of a MOS transistor and  $V_{DSsat}$  is the drain-source saturation voltage.

based on sensing the voltage across the current source and is independent of the type of the biased circuits. In the case where the proposed LV current source is used to bias a differential pair, it does not require a replica differential pair. This LV current source can also be used for other types of circuits such as source followers.

## II. CURRENT SOURCE STRUCTURE

### A. Principle of Operation

Fig. 1(a) shows the conceptual schematic of the proposed LV current source. The representation of the proposed structure is illustrated in Fig. 1(b). A constant current  $I_B$  (with a finite resistance  $R_{oB}$ ) is injected into  $M_1$  which is mirrored to the output transistor  $M_2$ . A change in  $V_x$  (the output voltage of the current source at node X) will force a similar change in  $V_y$  because of the virtual short circuit provided by the error amplifier A. This implies that the drain-to-source voltage of  $M_1$  tracks that of  $M_2$ . Since the drain current of  $M_1$  is fixed and is equal to  $I_B$ , the error amplifier adjusts the gate voltage to compensate for the change in the drain-to-source voltage of  $M_1$  and  $M_2$ . The output current remains fairly constant which implies that the effective resistance of  $M_2$  has been enhanced.

### B. Circuit Analysis

1) *Output Impedance of the Current Source:* For the current source in Fig. 1(a), a small signal equivalent circuit has been used to obtain the equivalent output impedance (seen at the drain of  $M_2$ ). The analysis shows that the output resistance at node X is given by

$$R_{os} = \frac{1 + g_{m1} A_o / (g_{o1} + g_{oB})}{g_{o2} (1 + A_o g_{m1} / (g_{o1} + g_{oB}) - A_o g_{m2} / g_{o2})} \quad (1)$$

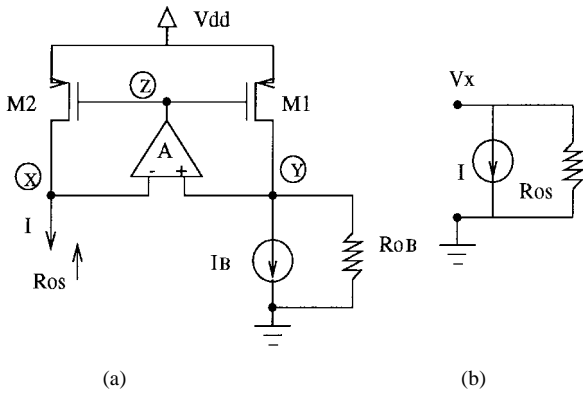


Fig. 1. A conceptual schematic of the low-voltage current source: (a) architecture and (b) current source representation.

where  $g_{m1}(g_{m2}), g_{o1}(g_{o2})$  are the transconductance and output conductance of  $M_1(M_2)$ , respectively.  $A_o$  is the dc gain of the error amplifier “A” and  $g_{oB}(R_{oB})$  is the output conductance (resistance) of the reference current source  $I_B$ . Assuming that there is a good match between transistors  $M_1$  and  $M_2$  so that  $g_{m1} = g_{m2}$  and  $g_{o1} = g_{o2}$ , (1) can be simplified as

$$R_{os} \approx -R_{oB}. \tag{2}$$

Note that the resistance is negative and is equal to the resistance of the reference source  $I_B$ .

The proposed realization of the current source is shown in Fig. 2. The error amplifier is implemented as a single-ended differential pair with a current mirror load. The reference current is realized as a cascode source ( $M_3$  and  $M_4$ ). Thus, the output resistance is

$$R_{os} \approx -\frac{g_{m4}}{g_{o3}g_{o4}} \tag{3}$$

where  $g_{m4}(g_{m3})$  and  $g_{o4}(g_{o3})$  are the transconductance and output conductance of  $M_4(M_3)$ , respectively. Note that if a regulated cascode or an active regulated cascode current source is used to implement the  $I_B$  source [1], [2], the output resistance of the LV current source will be in the order of  $g_m^2/g_o^3$ . The main strength of the proposed low-voltage current source is that its compliance voltage will always be less than one  $V_{DSsat}$ .

The proposed current source is meant to provide high output resistance as proven by the above dc analysis. A rigorous analysis for the output impedance at high frequencies is too complicated. Instead, we present a simplified analysis which yields a good approximation of the output impedance as a function of frequency.

At this point, it is important to recall that the high gain of amplifier A facilitates the virtual short circuit between nodes X and Y (see Fig. 1), which, in turn, causes the output resistance to track the resistance at node Y. At high frequency, however, this is no more the case because of the reduced gain of the amplifier. As a result, the output impedance (at node X) becomes gradually independent on that of node Y as the frequency increases.

The output impedance  $Z_{os}$  (at node X in Fig. 1) can be viewed, simply, as the parallel combination of  $R_{os}$  and  $C_x$ ,

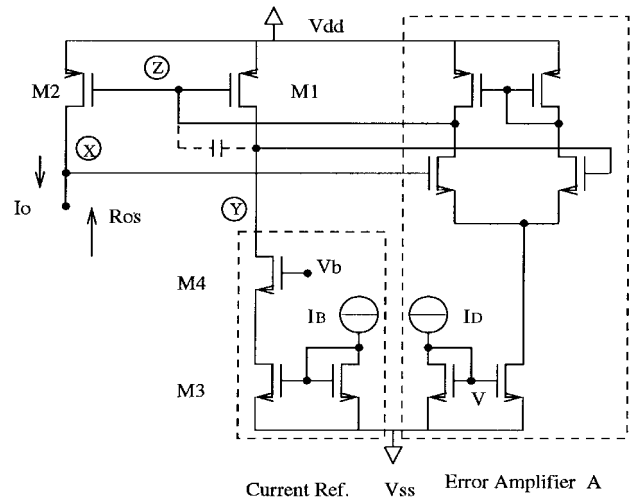


Fig. 2. Full implementation of the LV current source.

the parasitic capacitance at node X. At low frequencies,  $Z_{os}$  is equal to  $R_{os}$ , and at high frequencies  $Z_{os}$  is dominated by the impedance of the capacitance  $C_x$ . Simulation results, illustrated in Fig. 3 (curve a), show that the normalized impedance, which is defined as  $Z_{os}/R_{os}$ , is close to unity at low frequencies. As the frequency increases, the normalized impedance falls by a 20 dB/decade indicating that the impedance is capacitive. If the current source is used to provide tail current to a P-type differential pair, the behavior of the impedance at node X is similar to the previously discussed case, except that the impedance of the capacitance will become dominant at higher frequencies as demonstrated by the simulation results in Fig. 3 (curve b). The above analysis is not quite accurate, but yields good approximation of the actual impedance behavior and agrees well with the simulations.

2) *Stability Analysis:* The proposed LV current source consists of two loops; one with a negative feedback (consisting of the error amplifier A and M1) and the other with a positive feedback (A and M2). This may lead to instability especially if the positive feedback dominates the negative feedback. A detailed and rigorous stability analysis was conducted, and is presented here, to find the requirements for stability.

First, the analysis was based on the small signal equivalent circuit, shown in Fig. 4, without  $C_c$ . The following assumptions were made;  $g_{oB}$  is the conductance of current source  $I_B$ ,  $g_i$  is the conductance of the circuit biased by the LV current source, and  $C_x$  and  $C_y$  are the total parasitic capacitance at nodes  $x$  and  $y$ , respectively. It is also assumed that the error amplifier has a single dominant pole with the following transfer function:

$$A(s) = \frac{A_o}{1 + sC_z/g_{oa}} \tag{4}$$

where  $C_z$  is the capacitance at node  $z$  and  $g_{oa}$  is the output conductance of the amplifier, which will be in the order of  $g_o$  (see the implementation of the error amplifier in Fig. 2).

The stability of the LV current source can be tested using the open-loop transfer function. This was derived by opening the negative and positive loops at the inputs of the error amplifiers as shown in Fig. 4. The open-loop transfer function is defined

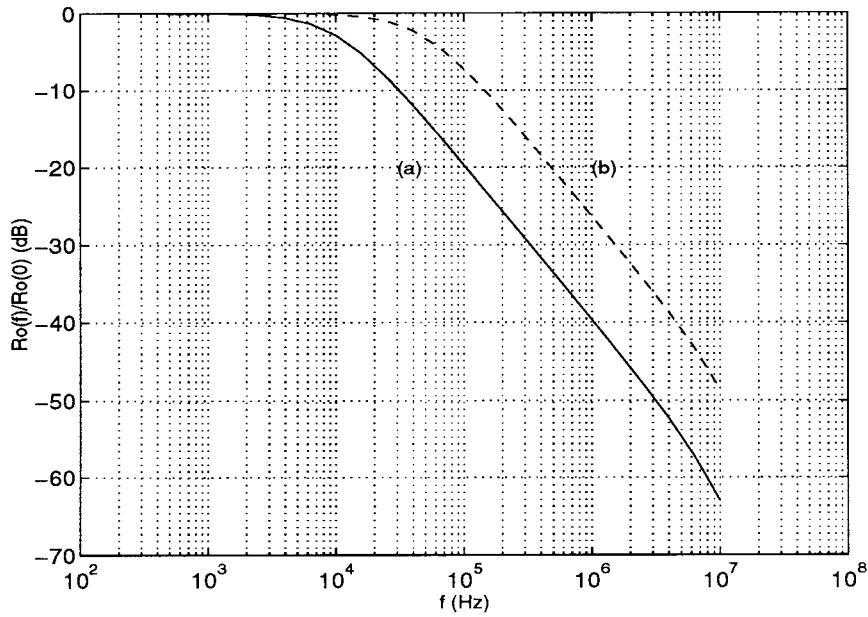


Fig. 3. Frequency response of the tail current output impedance (a) without differential pair and (b) with differential pair.

as

$$H_{OL} = \frac{v_o(s)}{v_i(s)}$$

It can be shown that

$$H_{OL}(s) = A_L^-(s) - A_L^+(s) \quad (5)$$

where  $A_L^-$  is the gain of the negative loop and is given by

$$A_L^- = \frac{A_o g_{m1} / (g_{o1} + g_{oB})}{(1 + sC_z / g_{oa})(1 + sC_y / (g_{o1} + g_{oB}))}$$

and  $A_L^+$  is the gain of the positive loop and is given by

$$A_L^+ = \frac{A_o g_{m2} / (g_{o2} + g_i)}{(1 + sC_z / g_{oa})(1 + sC_x / (g_{o2} + g_i))}$$

The  $g_{m1}(g_{m2})$  and  $g_{o1}(g_{o2})$  account for the transconductance and output conductance of  $M_1(M_2)$ . Equation (5) can be simplified as

$$H_{OL}(s) = \frac{A_o g_m (g_i - g_{oB})}{g_o (g_o + g_i)} \times \frac{1 + s(C_x - C_y) / (g_i - g_{oB})}{(1 + s/p_x)(1 + s/p_y)(1 + s/p_z)} \quad (6)$$

where

$$p_z = \frac{g_{oa}}{C_z}, \quad p_y = \frac{(g_o + g_{oB})}{C_y}, \quad p_x = \frac{(g_i + g_o)}{C_x}$$

Note that in deriving (6) it was assumed that  $g_{m1} = g_{m2} = g_m$  and that  $g_{o1} = g_{o2} = g_o$ .

Equation (6) indicates that the open-loop transfer function has three poles and one zero. Two of the poles,  $p_z$  and  $p_y$ , are close to each other. The location of the first pole  $p_x$  depends on the value of  $g_i$ . If the LV current source is used to provide the tail current of the differential pair (which is the most common application of the LV source) or is used to provide biasing

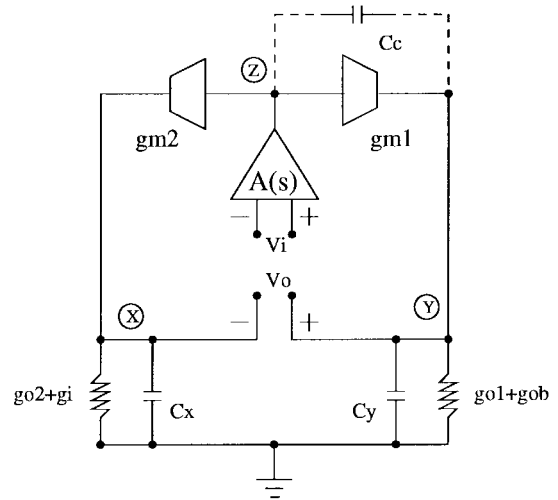


Fig. 4. Small signal model of the LV current source.

current for source followers, then  $g_i$  will be small (of the order of  $g_m$ ). The pole  $p_x$  will be much greater than the other two poles,  $p_y$  and  $p_z$ . Having these two poles in close proximity will probably lead to instability. This has been verified by the open-loop frequency response of the LV current source as shown in Fig. 5 curve (a), where phase margin is close to  $0^\circ$ . The poles  $p_z$  and  $p_y$  can be split by using a Miller compensation capacitance ( $C_c$ ) connected between nodes y and z as shown in Fig. 4. The open-loop transfer with the compensation capacitance in place is given by

$$H_{OL} = \frac{A_o g_m (g_i - g_{oB})}{(g_o + g_{oB})(g_o + g_i)} \times \frac{(1 - s/z_1)(1 + s/z_2)}{(1 + s/p_x)(1 + s/p'_y)(1 + s/p'_z)} \quad (7)$$

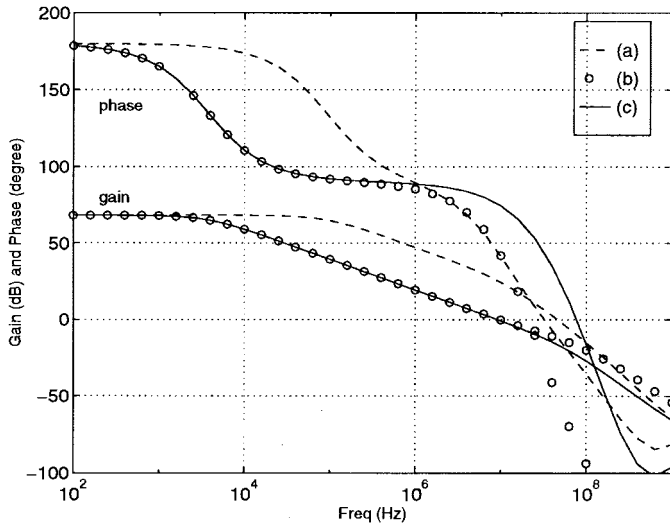


Fig. 5. Open-loop frequency response of the tail current source.

where

$$z_1 = \frac{g_i - g_{oB}}{C_c} \times \frac{g_m}{g_m + g_i}$$

$$z_2 = \frac{g_m}{C_y}$$

$$p'_y = \frac{g_m}{C_y + C_x}$$

$$p'_z = \frac{g_{oa}g_o}{g_m C_c}$$

The pole splitting causes  $p_z$  to become the dominant pole,  $p'_z$ , while  $p_y$  moves to a higher frequency (compare the expressions of  $p_y$  and  $p'_y$ ). The pole  $p_x$  will not be affected by adding the compensation capacitance. Thus, its impact on the phase margin will be insignificant. It can be observed that  $p_x$  will be comparable to  $p'_y$ . Assuming that  $g_{oB} \ll g_o$  [see (3)] and that  $g_i \gg g_o$  ( $g_i \simeq g_m$ ), the gain-bandwidth (GBW) product can be approximated by

$$\text{GBW} \simeq \frac{g_{ma}}{C_c} \times \frac{g_i}{g_o + g_i} \simeq \frac{g_{ma}}{C_c} \quad (8)$$

where  $g_{ma}$  is the transconductance of the error amplifier and is given by

$$g_{ma} = A_o g_{oa}$$

The effect of the Miller capacitance has been verified through the simulation. Curve (b) in Fig. 5 demonstrates that a  $45^\circ$  phase margin can be achieved by using a 1-pF compensation capacitance  $C_c$ . Since the LV current source will be mainly used to provide tail current for circuits with low input impedance, such as the differential pairs,  $g_i$  will be of the order of  $g_m$ . This implies that  $z_1$ , which is a right-half plane (RHP) zero, will be close to the unity gain frequency, thus causing significant reduction in the phase margin. To overcome this problem, a resistance  $R_c$  can be added in series with  $C_c$  to push  $z_1$  to higher frequencies (as is the case for the conventional two-stage CMOS amplifier). It can be shown

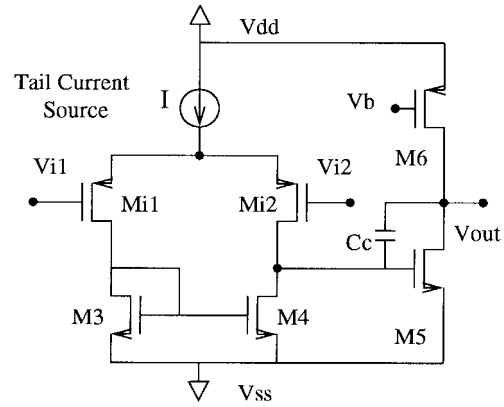


Fig. 6. The two-stage amplifier used to test the effect of the LV source on its frequency response.

that  $z_1$  will become

$$z_1 = \frac{1}{C_c(1/g_m + 1/g_i - R_c)}$$

The effect of  $R_c$  can be observed from curve (c) in Fig. 5, where the phase margin is greater than that of curve (b).

To test the impact of the frequency response of the LV current source on the performance of the circuit to be biased by the proposed current source, we use the two-stage amplifier shown in Fig. 6. The frequency response of this amplifier was simulated for two cases; first with a simple transistor tail current source and second with the proposed LV current source. The simulation was performed using HSPICE. The frequency response of the two-stage amplifier for both cases is shown in Fig. 7. The solid line shows the frequency response of the amplifier with a simple current source. The dashed line represents that with the LV current source. It is observed that LV source does not cause degradation in the frequency response of the amplifier. The GBW of the two stage amplifier is predominantly determined by its output load capacitance. Hence, it is not affected by the LV current source. A slight reduction in the phase at frequencies well above the unity-gain frequency is observed.

### C. Experimental Results

The LV current source in Fig. 2 has been fabricated in the 2- $\mu\text{m}$  CMOS Orbit process (through MOSIS). The same circuit has been used as a simple current source by connecting node Z to Y and connecting node V to  $V_{ss}$  (to disable the error amplifier A). The aspect ratios of  $M_1$  and  $M_2$  are  $200 \mu\text{m}/3 \mu\text{m}$ . Fig. 8 illustrates the measured current sourced by both circuits. Note that the slope of curve A (of the simple current source) is larger than that of curve B (of the LV source). The output resistance of the simple current source is  $320 \text{ k}\Omega$ , while that of the new LV source is  $8 \text{ M}\Omega$  (a factor of 25 improvement in the resistance). The positive slope of curve B implies that the resistance of the LV current source is negative, which was predicted by the analysis [see (1)]. The compliance voltage varies from 120 mV at  $20 \mu\text{A}$  to 300 mV at  $90 \mu\text{A}$  (see Fig. 9). In comparison, the compliance voltage of the simple current source is 200 mV at  $20 \mu\text{A}$  and 400 mV at  $90 \mu\text{A}$ .

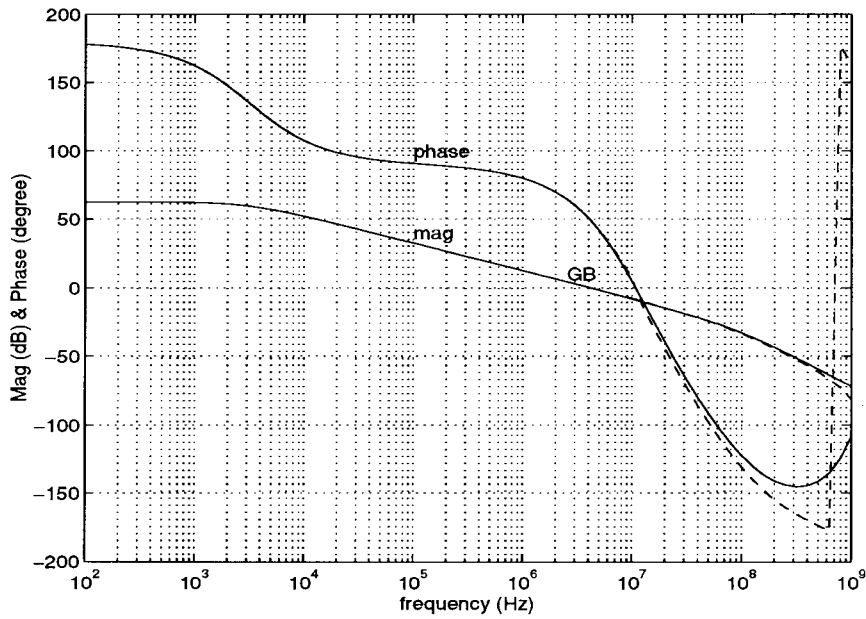


Fig. 7. Frequency response of two-stage amplifiers using LV current source (dashed) and simple current source (solid).

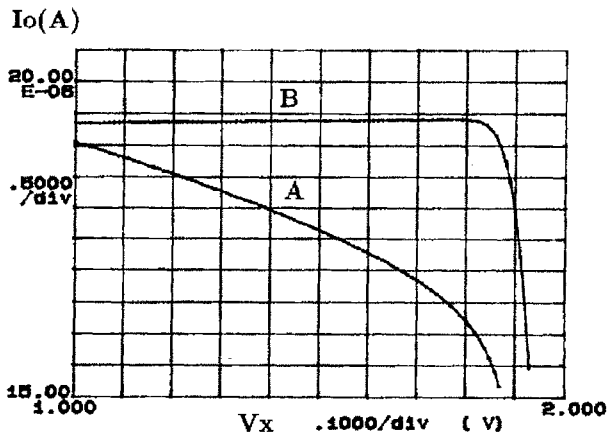


Fig. 8. Measured output current of the simple current source (curve A) and LV current source (curve B).

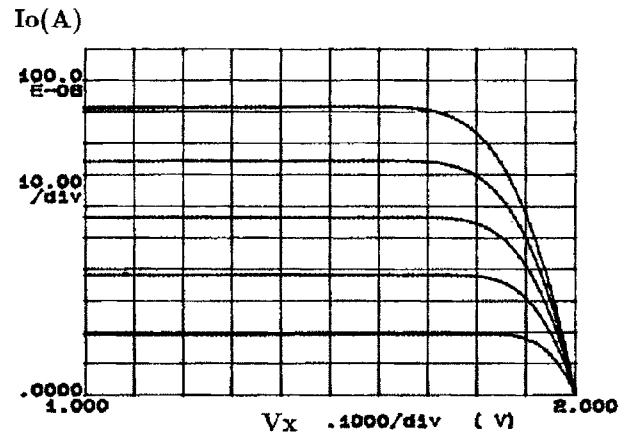


Fig. 9. Measured I-V characteristics of the LV current source.

### III. USING THE LV CURRENT SOURCE FOR LOW VOLTAGE DIFFERENTIAL AMPLIFIERS

The proposed current source is well suited for low-voltage differential amplifiers. The increased output resistance of the source with its small compliance voltage improves the common-mode rejection ratio (CMRR) and the input CMR.

#### A. Single-Ended (SE) Differential Amplifiers

1) *Circuit Analysis*: A detailed small signal analysis for the SE amplifier, shown in Fig. 10(a), has been carried out. The mismatching between  $M_{i1}$  and  $M_{i2}$  is accounted for by assuming that  $g_{mi1} = g_{mi}(1 + \epsilon_i/2)$  and  $g_{mi2} = g_{mi}(1 - \epsilon_i/2)$ . Similarly, for the load transistors  $M_3$  and  $M_4$ ,  $g_{m3} = g_{ml}(1 + \epsilon_l/2)$  and  $g_{m4} = g_{ml}(1 - \epsilon_l/2)$ . The common-mode gain for the SE differential amplifier has been derived in terms of its systematic and random components  $A_{cs}$  and  $A_{cr}$ , respectively

$$A_{cs} = \frac{-g_{os}}{2g_{ml}} \quad (9)$$

$$A_{cr} = \frac{\epsilon(g_{oi} + g_{os})}{g_{oi} + g_{ol}} \quad (10)$$

where  $g_{oi}$  and  $g_{ol}$  are the output conductances of  $M_{i1}$  ( $M_{i2}$ ) and  $M_3$  ( $M_4$ ), respectively. Recall that  $g_{os}$  is the output conductance of the tail current source. For simplicity, we have assumed that  $\epsilon_i = \epsilon_l = \epsilon$ . The common-mode gain components of the SE differential amplifier using the simple current source have been compared with those of an SE differential amplifier with an LV current source (see Table II). For the case of the simple current source,  $g_{os}$  is comparable to  $g_{oi}$  and  $g_{ol}$ . Hence, the random common-mode gain is in the order of  $\epsilon$ . If  $\epsilon$  is 1%, the systematic common-mode gain dominates over the random gain. For the LV current source,  $g_{os}$  is in the order of  $g_o^2/g_m$ . Thus, the random common-mode gain is the dominant component (see Table II). The use of the LV current source reduces the common-mode gain by about four (if  $g_m/g_o = 25$  and  $\epsilon = 1\%$ ). This translates into a 12 dB increase in the CMRR.

2) *Experimental Results*: The measured output voltage of the SE differential amplifier versus the common-mode input

TABLE II  
IMPACT OF THE SIMPLE AND LV SOURCE ON  $A_c$ ,  $A_{dc}$ ,  $A_{cc}$

		Simple CS $g_{os} = g_o$	LV CS $g_{os} = g_o^2/g_m$	$\frac{A_{simple}}{A_{LV}}$
SE	$A_{cs}$	$-g_o/2g_m$	$g_o^2/g_m^2$	$g_o/\epsilon g_m$
	$A_{cr}$	$\epsilon$	$\epsilon/2$	$(\approx 12 \text{ dB})$
	$A_c$	$-g_o/2g_m$	$\epsilon/2$	
FB	$A_{dc}$	$1.5\epsilon$	$0.5\epsilon$	$3 (\approx 10 \text{ dB})$
	$A_{ccs}$	$0.5$	$g_o/g_m$	$g_m/g_o \approx 10$
	$A_{ccr}$	$\epsilon/4$	$\epsilon/4$	$(20 \text{ dB})$
	$A_{cc}$	$0.5$	$g_o/g_m$	

Each entry gives the order of magnitudes of  $A_c$ ,  $A_{dc}$  and  $A_{cc}$  in terms of  $\epsilon$  and  $g_m/g_o$  ( $\epsilon < 1\%$ ,  $g_m/g_o = 25$ )

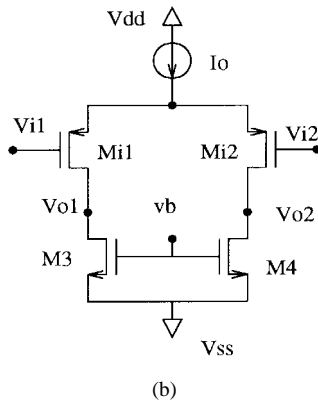
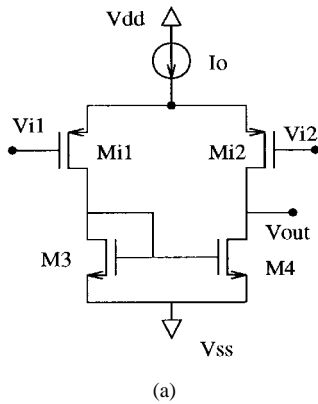


Fig. 10. Schematics of differential amplifiers: (a) single-ended and (b) fully balanced.

is shown in Fig. 11. Curve A corresponds to the SE differential pair with the simple current source, while B corresponds to that with the LV source. The slopes of the linear portions of the curves can be used as a measure for the common-mode gain. From the figure it is observed that the LV source reduces the common-mode gain by a factor of five, which means that the CMRR improves by 14 dB (as predicted by the analysis). It is also important to mention that  $\epsilon$  was measured to be slightly less than 1%.

### B. Fully Balanced (FB) Differential Amplifiers

1) *Circuit Analysis*: First, recall the following equations for the differential and common-mode output voltages of an

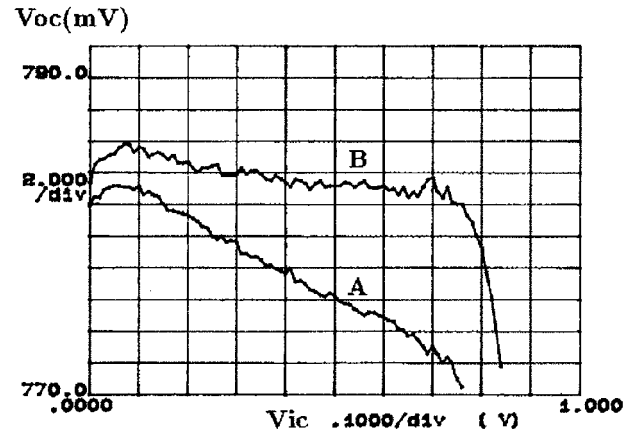


Fig. 11. Measured output voltage versus common-mode input voltage for an SE amplifier with simple current source (curve A) and LV current source (curve B).

FB pair [Fig. 10(b)] [6]:

$$v_{od} = A_{dd}v_{id} + A_{dc}v_{ic} \quad (11)$$

$$v_{oc} = A_{cd}v_{id} + A_{cc}v_{ic} \quad (12)$$

where  $v_{id}$  and  $v_{ic}$  are defined as the differential and common-mode input voltages, respectively. Both types of common-mode gains  $A_{dc}$  and  $A_{cc}$  have been derived. The first is only due to random mismatch and is given by

$$A_{dc} = \epsilon \frac{g_{oi}g_{ol} + g_{os}(g_{oi} + g_{ol})}{g_{ol}(g_{oi} + g_{ol})} \quad (13)$$

Table II shows that the common-mode gain  $A_{dc}$  of the FB differential amplifier, with the LV current source, is a factor of three smaller than that of the same amplifier with a simple current source. This implies that the CMRR of the FB differential amplifier, which is defined as  $A_{dd}/A_{dc}$ , improves by 10 dB if the proposed LV current source is used instead of the simple one.

The common-mode gain  $A_{cc}$  consists of the following systematic and random components:

$$A_{cs} = \frac{g_{os}}{2g_{ol}} \quad (14)$$

$$A_{cr} = \frac{\epsilon g_{ol}}{2(g_{oi} + g_{ol})} \quad (15)$$

Assuming that  $\epsilon < 1\%$ , the systematic component dominates when both types of current sources are used (see Table II). Yet, in the case of the simple current source, the value of  $A_{cc}$  is higher than that of the LV current source by a factor of ten which corresponds to 20 dB reduction in  $A_{cc}$ .

2) *Experimental Results*: Fig. 12 shows the measured differential output voltages ( $V_{od}$ ) of the FB differential amplifier with the simple current source (curve A) and with the LV current source (curve B). Two observations can be made. First, the input CMR of the amplifier with the simple current source is between 250 mV and 650 mV, while that of the LV current source is between 250 mV and 870 mV. A 200-

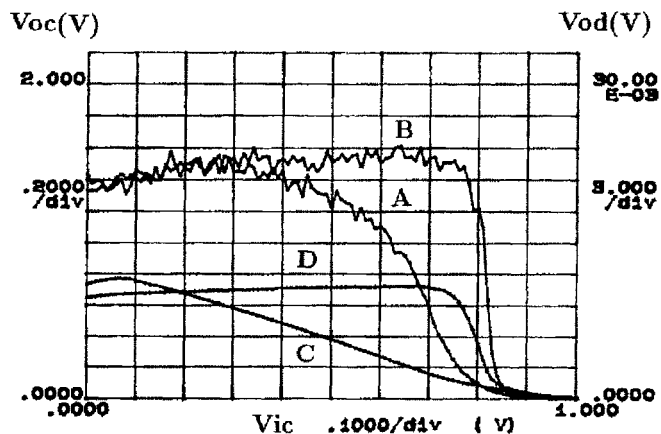


Fig. 12. Measured  $V_{oc}$  and  $V_{od}$  versus common-mode input for the FB amplifier with simple current source (curves A and C) and LV current source (curves B and D).

mV increase in the CMR is significant for low-power supply voltages. For the 2 V supply used in our measurements, the CMR improves by 10%. To compare the values of  $A_{dc}$  one can measure the slopes of both curves in the valid input range. While it is difficult to measure exact values for the slopes because of the measurement's resolution, one can show that the LV current source results in a reduction of  $A_{dc}$  by a factor of six (15 dB). Curves C and D in Fig. 12 show the measured common-mode outputs ( $V_{oc}$ ) of the FB amplifiers with the simple and the LV sources, respectively. The dramatic improvement of  $A_{cc}$ , which is predicted by the analysis, has been confirmed by comparing the slopes of curves C and D. The improvement of  $A_{cc}$  is measured to be 31 dB. The fact that the common-mode output voltages are well controlled through the use of the LV current source relaxes the requirement of the common-mode feedback loop needed to stabilize the common-mode component in the feedback amplifier.

#### IV. CONCLUSION

A new low-voltage current source has been proposed. This source offers both high output resistance (8 M $\Omega$ ) and low compliance voltage (200 mV). We have demonstrated that the proposed current source improves the input common-mode range and the common-mode rejection ratio of low voltage differential amplifiers. The analysis has shown, however, that the CMRR of single-ended and fully balanced differential amplifiers will be eventually limited by the process mismatching when the output resistance of the tail current source is increased. The new LV current source provides very good control over the common-mode output of the fully balanced amplifiers, which allows for simple common-mode feedback circuits.

#### ACKNOWLEDGMENT

The authors would like to acknowledge the reviews for their valuable comments.

#### REFERENCES

- [1] E. Sackinger and W. Guggenbuhl, "A high-swing, high-impedance MOS cascode circuit," *IEEE J. Solid-State Circuits*, vol. 25, pp. 289–298, Jan. 1990.
- [2] P. J. Crawley and G. W. Roberts, "High-swing MOS current mirror with arbitrarily high output resistance," *Electron. Lett.*, vol. 28 no. 4, pp. 361–363, Feb. 1992.
- [3] T. Serrano and B. Linares-Barranco, "The active-input regulated-cascode current mirror," *IEEE Trans. Circuits Syst.*, vol. 41, pp. 464–467, June 1994.
- [4] W. Krenik, *et al.*, "High dynamic range CMOS amplifier design in reduced supply voltage environment," in *Tech. Dig. Midwest Symposium on Circuits and Systems*, 1988, pp. 368–370.
- [5] F. You, S. H. K. Embabi, J. Duque-Carrillo, and E. Sánchez-Sinencio, "An improved current source for low voltage application," in *IEEE Custom Integrated Circuits Conf.*, May, 1996, pp. 97–100.
- [6] P. R. Gray and R. G. Meyer, *Analysis and Design of Analog Integrated Circuits*. New York: Wiley, 1984.



designs for multimedia applications.

**Fan You** received the B.S. degree from Tsinghua University, Beijing, China, in 1985, the M.S. degree from Louisiana State University, Baton Rouge, in 1991, and the Ph.D. degree from Texas A&M University, College Station, in 1996.

From 1993 to 1996, he worked with the Microelectronics Group at Texas A&M University as a Research Assistant in the area of low-voltage analog circuit design. He is currently a Member of Technical Staff in the Bell Labs of Lucent Technologies, Allentown, PA, where he is working on VLSI



**Sherif H. K. Embabi** (S'87–M'91) received the B.Sc. and M.Sc. degrees in electronics and communications from Cairo University, Egypt, in 1983 and 1986, respectively, and the Ph.D. degree in electrical engineering from the University of Waterloo, Canada, in 1991.

In 1991, he joined Texas A&M University, College Station, as an Assistant Professor of Electrical Engineering. In the academic year 1996/97, he has been on a leave of absence with Texas Instruments in Dallas, Texas. His research interests are in the area of VLSI implementations of mixed-signal systems. He has worked on BiCMOS digital circuit design. Currently, his interests are in the area of low-voltage analog circuit design, field programmable analog arrays, and RF circuits.

Dr. Embabi is a co-author of *Digital BiCMOS Integrated Circuit Design* (Kluwer, 1993). He is the recipient of an NSF Research Initiation Award in 1994. He is currently serving as an Associate Editor for the IEEE TRANSACTIONS ON CIRCUITS AND SYSTEMS (PART II).



**J. Francisco Duque-Carrillo** (M'86) received the M.Sc. degree in electronic physics from the University of Sevilla, Sevilla, Spain, and the Ph.D. degree from the University of Extremadura, Badajoz, Spain, in 1979 and 1984, respectively.

In 1986 and 1987, on a NATO Fellowship, he was a Visiting Scholar at the Electrical Engineering Department of Texas A&M University, College Station. In 1988, he was with AT&T Microelectronics in Madrid, Spain, and Allentown, PA. Currently, he is with the University of Extremadura where he holds a Professor position. His research interests focus on the area of analog and mixed-mode integrated circuit design for signal and neural information processing.



**Edgar Sánchez-Sinencio** (S'72-M'74-SM'83-F'92) received the M.S.E.E. degree from Stanford University, Stanford, CA, and the Ph.D. degree from the University of Illinois at Champaign-Urbana in 1970 and 1973, respectively. He did an industrial postdoctoral with Nippon Electric Company, Kawasaki, Japan, in 1973-1974.

Currently, he is with the Department of Electrical Engineering, Texas A&M University, as a Professor. He is the co-author of *Switched-Capacitor Circuits* (Van Nostrand-Reinhold, 1984)

and co-editor of *Artificial Neural Networks: Paradigms, Applications, and Hardware Implementations* (IEEE Press, 1992). His research interests are in the area of solid-state and RF-circuit implementations.

Dr. Sánchez-Sinencio has been the Guest Editor or Co-Editor of three special issues on Neural Network Hardware (IEEE TRANSACTIONS ON NEURAL NETWORKS, March 1991, May 1992, May 1993) and one special issue on Low Voltage Low Power Analog and Mixed-Signal Circuits and Systems (IEEE TRANSACTIONS ON CIRCUITS AND SYSTEMS I, November 1995). He was the IEEE/CAS Technical Committee Chairman on Analog Signal Processing (1994-1995). He has been Associate Editor for different IEEE magazines and transactions from 1982 until now. He was the IEEE Video Editor for the IEEE TRANSACTIONS ON NEURAL NETWORKS. He was also the IEEE Neural Network Council Fellow Committee (1990-1992). He was the 1993-1994 IEEE Circuits and Systems Vice President-Publications and a member of the IEEE Press Editorial Board. In 1995, he received an Honoris Causa Doctorate from the National Institute for Astrophysics, Optics and Electronics, Puebla, Mexico. In 1992 he was elected as a Fellow of the IEEE for contributions to monolithic analog filter design.